

REGULATION OF NITRIC OXIDE EMISSIONS FROM FOREST AND RANGELAND SOILS OF WESTERN NORTH AMERICA

JOHN M. STARK,^{1,3} DAVID R. SMART,^{1,4} STEPHEN C. HART,² AND KAREN A. HAUBENSAK^{2,5}

¹Department of Biology, and the Ecology Center, Utah State University, Logan, Utah 84322-5305 USA

²School of Forestry, College of Ecosystem Science and Management, Merriam-Powell Center for Environmental Research, Northern Arizona University, Flagstaff, Arizona 86011-5018 USA

Abstract. Nitric oxide (NO) is a relatively short-lived trace gas that reacts with oxygen in the troposphere to produce the air pollutant ozone. It also reacts with water vapor to form nitric and nitrous acids, which acidify precipitation and increase N deposition. Models currently used to predict soil NO fluxes are based on the assumption that NO flux is proportional to the gross rate of nitrification or N mineralization; however, this assumption has not been tested because of the difficulty in measuring gross N-cycling rates in situ. We measured soil NO fluxes, gross and net N-cycling rates, and a variety of other soil characteristics in the forest floor and intact soil cores at nine undisturbed forest and rangeland ecosystems of New Mexico, Utah, and Oregon, USA, to determine which soil variables were most closely related to soil NO flux. Soil NO fluxes ranged from a low of 0.02 ng N·m⁻²·s⁻¹, prior to wetting in a western hemlock–sitka spruce forest on the Oregon coast, to a high of 6.74 ng N·m⁻²·s⁻¹, one hour after soil wetting in a juniper woodland of central Oregon. In contrast to our expectations, neither gross nitrification nor gross mineralization was correlated with soil NO flux. Fluxes were positively correlated with net rates of mineralization and nitrification, soil NO₃⁻ concentrations, bulk density, and pH, and negatively correlated with gross rates of NO₃⁻ consumption in the forest floor, soil organic carbon (SOC), soil C:N, and soil water content. Principal-component analysis showed that NO flux after water addition (2 cm of water) had a strong negative correlation with microbial demand for N (as indicated by net mineralization, net nitrification, SOC, and C:N). Our results suggest that, even in well-drained soils, NO efflux is limited more by NO consumption than by NO production. As a result, models utilizing the more easily measured net rates, rather than gross rates, may be better predictors of soil NO fluxes across a range of ecosystems.

Key words: gross N-cycling rates; isotope dilution; modeling; ¹⁵N; N mineralization; nitrification; nitrogen; Oregon Transect Ecosystem Research (OTTER) transect; sagebrush; soil organic matter; temperate forests; trace N gas.

INTRODUCTION

Soil production of the trace nitrogen gas nitric oxide (NO) has received increasing attention over the past two decades, because this gas has significant adverse environmental effects. Nitric oxide is a relatively short-lived trace gas that reacts with O₂ in the troposphere to produce the air pollutant ozone (O₃) (Logan 1983). It also reacts with water vapor to form nitric and nitrous acids, which acidify precipitation and increase N deposition. Attempts to develop regional and global budgets for trace gases have been hampered by the limited amount of information on NO fluxes from many ecosystems. For example, in a recent literature review, Davidson and Kinglerlee (1997) found only four esti-

mates of NO fluxes from temperate forest ecosystems. Attempts to model trace N gas fluxes have also had limited success, because we lack mechanistic information on what controls trace gas flux from soils in a variety of ecosystems (Matson 1997, Venterea and Rolston 2000).

One of the difficulties encountered when modeling trace gas flux is that the gas production may result from several different processes. Autotrophic nitrification is the primary source of NO in most well drained soils (Anderson et al. 1988, Bollmann and Conrad 1998, Godde and Conrad 1998, Smart et al. 1999, Wolf and Russow 2000); however, at low pH, heterotrophic nitrification (Papen et al. 1989) or autodecomposition of nitrite may be significant NO sources (Firestone and Davidson 1989, Conrad 1996). In soils with poor aeration, denitrification may also produce small amounts of NO (Conrad 1996).

The most widely used conceptual model of trace N gas flux from soils is the “hole-in-the-pipe” model proposed by Firestone and Davidson (1989) (Fig. 1). This model suggests that trace N gas production in soil

Manuscript received 26 April 2001; revised 8 October 2001; accepted 10 October 2001; final version received 19 December 2001.

³ E-mail jstark@biology.usu.edu

⁴ Present address: Department of Viticulture and Enology, University of California, Davis, California 95616-8749 USA.

⁵ Present address: Department of Integrative Biology, University of California, Berkeley, California, USA.

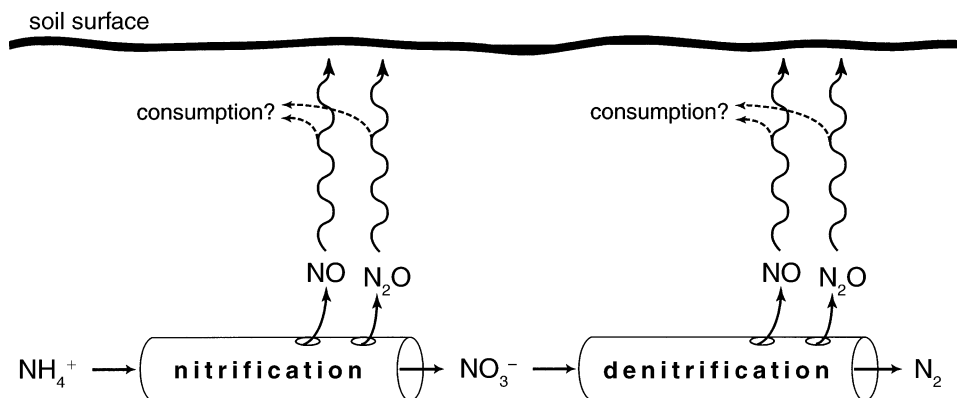


FIG. 1. "Hole-in-the-pipe" conceptual model of trace N gas production in soil. Modified from Firestone and Davidson (1989).

is regulated at three levels. The first is the "flow through the pipe," or the gross rates of nitrification and denitrification, the two microbial processes that produce NO and nitrous oxide (N_2O). Factors that increase gross nitrification or denitrification rates are predicted to increase trace N gas flux. The second level of regulation is the "size of the holes in the pipes." These "holes" represent the factors that control partitioning of N among the end products. Such factors include the relative availability of oxidants (O_2 , NO_3^-) and reductants (reduced carbon compounds), temperature, pH, as well as factors that might uncouple intermediate compounds from enzymes or otherwise prevent nitrification and denitrification from progressing to completion. Once NO is produced in a soil microsite, it must move to the soil surface before it can be emitted. Therefore, transport processes represent a third level of regulation of trace-gas production. As the volume of water-filled pore space (WFPS) in soil decreases, diffusion and transport of gases increase. Upward movement of NO, N_2O , and other gases produced in soils should thus increase as soil water content declines. Transport of O_2 into the soil will also increase, however, which may slow production rates of trace N gases. The net effect of increased WFPS on NO flux will depend on the balance between transport of NO out of the soil and how O_2 influences nitrification, denitrification, and partitioning of N among gaseous products. Davidson (1991) hypothesized that the fraction of WFPS in soil would control the relative amounts of NO, N_2O , and N_2 , where at WFPS <0.6 , NO would dominate because of rapid nitrification (which produces a high value of the ratio NO: N_2O) and high transport rates. At WFPS levels ranging from 0.6 to 0.9, N_2O would dominate, because moderately low O_2 tensions would lower the ratio NO: N_2O produced during nitrification, but increase the ratio N_2O : N_2 produced during denitrification; and at WFPS >0.9 , N_2 would predominate, because an absence of O_2 would prevent nitrification and lower the ratio N_2O : N_2 produced during denitrification.

A fourth level of regulation of NO emission, which

is not specifically addressed by the hole-in-the-pipe model, is consumption by soil microorganisms (Davidson 1991). As NO diffuses through the soil solution and gaseous phase, denitrifying bacteria in anaerobic microsites may use NO as a terminal-electron acceptor during electron transport (Firestone and Davidson 1989). There is also evidence that NO may be oxidized to NO_2^- and NO_3^- in aerobic soil microsites (Baumgartner et al. 1996, Rudolph et al. 1996, Dunfield and Knowles 1997). While soils exposed to high NO concentrations have been shown to be sinks for NO, only a few coarse-scale models have considered consumption of NO to be an important regulator of soil NO flux (e.g., Otter et al. 1999).

Most recent simulation models designed to predict trace N gas emissions from soils assume that trace N gas production is a constant fraction of gross N-cycling rates (gross mineralization or gross nitrification), and that the relative partitioning of N among gaseous products is a function of WFPS, following a relationship similar to that described by Davidson (1991). For example, Potter et al. (1996, 1997) used the Carnegie-Ames-Stanford model to simulate coarse-scale soil NO and N_2O emissions, and assumed that trace N gas fluxes were equal to one percent of gross mineralization rates. However, they concluded that this percentage was a critical variable in the model, and that predictions might have been improved if the model had distinguished gross nitrification rates from gross mineralization rates. In a model by Parton et al. (2001), N_2O production is two percent of the gross nitrification rate and a variable portion of the denitrification rate. Nitric oxide production is then calculated based on a NO: N_2O ratio that changes with WFPS and soil pore size distribution.

Very few researchers have actually examined the relationships between trace N gas flux and gross nitrification rates. A number of studies have found that NO and N_2O fluxes are correlated with net mineralization rates, net nitrification rates, or soil NO_3^- concentrations (Robertson and Tiedje 1984, Matson and Vitousek

TABLE 1. Characteristics of study sites, and NO flux rates before, five minutes after, and one hour after addition of 2 cm of water to soil surface.

Ecosystem species	Sym- bol	pH [†]	Inorganic N [‡] (mg N/m ²)		N cycling (mg N·m ⁻² ·d ⁻¹) [§]			NO flux (ng N·m ⁻² ·s ⁻¹)		
			NH ₄ ⁺	NO ₃ ⁻	Gross nitrifi- cation	Net nitrifi- cation	Net mineral- ization	Ambi- ent	5 min	1 h
Oregon transect										
Western juniper (<i>Juniperus occidentalis</i>)	J	5.9	300	110	127	50	233	0.52	3.01	6.74
Ponderosa pine (<i>Pinus ponderosa</i>)	O	5.5	330	38	88	-78	-201	0.26	0.43	0.29
Mountain hemlock-pacific silver fir (<i>Tsuga mertensiana</i> - <i>Abies amabilis</i>)	M	4.8	170	20	199	-84	-49	0.07	0.99	0.05
Douglas-fir (<i>Pseudotsuga menziesii</i>)	D	5.0	230	80	156	88	1091	0.14	3.08	3.48
Western hemlock-sitka spruce (<i>Tsuga heterophylla</i> - <i>Picea sitchensis</i>)	H	3.8	360	2	173	26	-53	0.02	0.02	0.07
Tesuque watershed, New Mexico										
Pinyon pine/juniper (<i>Pinus edulis</i> / <i>Juniperus osteosperma</i>)	Y	6.1	310	130	24	-33	-4	0.31	2.02	2.14
Mixed conifer (<i>P. menziesii</i> / <i>Abies concolor</i>)	C	5.1	650	51	72	-41	-67	0.36	1.18	1.44
Aspen (<i>Populus tremuloides</i>)	A	5.1	830	38	64	-34	-106	0.58	0.22	0.32
Northern Utah										
Big sagebrush (<i>Artemisia tridentata</i>)	S	6.5	390	94	324	52	143	1.11	1.68	2.93

[†] Soil pH was measured in 0.01 mol/L CaCl₂ (2:1 solution : soil ratio).

[‡] The table presents 2 mol/L KCl-extractable N for the forest floor and 0–15 cm mineral soil layers combined.

[§] N-cycling rates are the sum of rates in the forest floor and 0–15 cm mineral soil layers.

1987, Williams et al. 1988, Verchot et al. 1999, Davidson et al. 2000, Hartley and Schlesinger 2000). These correlations have been taken as evidence that emissions are a function of gross nitrification rates (Davidson and Schimel 1995, Riley and Vitousek 1995, Verchot et al. 1999, Davidson et al. 2000); however, to truly evaluate the hole-in-the-pipe model, gross nitrification rates rather than net nitrification or mineralization must be measured, because it is gross nitrification that represents the flow through the first part of the pipe. Such data are limited, because measurement of gross N-cycling rates requires use of the ¹⁵N isotope dilution technique, which is considerably more difficult and time consuming than techniques used to measure net rates (Hart et al. 1994).

We are aware of only three field studies where gross nitrification rates were measured along with trace gas fluxes. Davidson et al. (1993a) measured gross rates along with NO and N₂O fluxes at two sites in a seasonally dry tropical forest in southern Mexico and calculated that, on average, trace N gas flux at this site was 0.01–0.1% of the gross N mineralization rate. Davidson et al. (1993b) also measured rates beneath oak canopies and in open grassy areas in adjacent grazed and ungrazed pastures of a California annual grassland. Grazed plots beneath oaks had the highest mean rate for both NO flux and gross nitrification; however, there was no relationship between NO flux and gross nitrifi-

cation among means from the other three locations. Within this site, NO fluxes ranged from 0.04% to 0.13% of gross nitrification rates. Riley and Vitousek (1995) measured trace N gas production and gross N-cycling rates in five Hawaiian montane rain forests. Unfortunately, consistent NO production was measured at only one of the sites, so NO flux could not be correlated with gross N-cycling rates or other soil characteristics. At the site where NO flux was detectable, NO flux was 0.03% of the gross N mineralization rate and 0.19% of gross nitrification.

In the current paper, we relate NO fluxes with soil C- and N-cycling characteristics across a wide range of forest and rangeland ecosystems of the western USA. We measured short-term NO fluxes and gross rates of nitrification, N mineralization, and inorganic N consumption, along with a variety of other soil characteristics. Our objective was to determine whether the gross nitrification rate is the most important soil variable determining NO emissions, and, if not, what other soil characteristics might be more predictive.

METHODS

Study sites

Nine sites in New Mexico, Oregon, and Utah were selected that represent a wide range of relatively undisturbed forest and rangeland ecosystems common in the western USA (Table 1; Stark and Hart 1997). In

mid-June 1993, NO fluxes, C- and N-cycling rates, and other soil characteristics were measured in pinyon-juniper, mixed conifer, and aspen forests in the Tesuque Watershed, 10 km north of Santa Fe, New Mexico. Soils of these ecosystems were formed from granitic parent materials and occur along an elevational transect ranging from 2400 to 3110 m elevation (Gosz 1980, Vitousek et al. 1982). In mid-August, measurements were made at five sites associated with the Oregon Transect Ecosystem Research project (OTTER transect; Gholz 1982, Runyon et al. 1994). This transect consists of a series of sites extending eastward from the Oregon coast to central Oregon, within 44–45° N latitude. Parent material for soil at the coastal site (western hemlock/sitka spruce) is marine derived siltstone and shale, while soils of the interior sites are derived from volcanic ash and basalt. In early September, measurements were made at a sagebrush-steppe community in northern Utah (Smart et al. 1999), located on soils formed in aeolian deposits. This series of nine sites spans almost the entire range of aboveground net primary production occurring in North America ($1\text{--}13\text{ Mg}\cdot\text{ha}^{-1}\cdot\text{y}^{-1}$; Gholz 1982).

Within each site, a 0.5-ha area was selected that was free of visible disturbance. Five locations were randomly chosen within this area for quantifying gross and net N-cycling rates and other soil characteristics. A 5×5 m plot was selected in the center of the 0.5-ha area for trace gas flux measurements.

Nitric oxide flux measurements

Fluxes of NO and NO₂ from the soil surface were measured using soil covers connected to a chemiluminescent NO₂ detector (Scintrex, NO₂ analyzer, model LMA-3, Concord, Ontario, Canada) in a configuration similar to that described by Davidson et al. (1991). In this detector, a CrO₃ filter was used to convert NO in the air stream to NO₂. The NO₂ reacts with a luminol solution and produces chemical luminescence, which is quantified using a photomultiplier tube. Four to eight polyvinyl chloride (PVC) rings (diameter, 25.5 cm; height, 12.0 cm) with beveled lower edges were placed on the forest floor surface. Fibrous forest floor material was cut with a knife around the perimeter of each ring so that the lower edge of the ring would contact the mineral soil. The ring was gently rotated and pressed into the mineral soil to a depth of ~1 cm. The rings were installed 2.5–4.0 h before the first measurement to minimize potential disturbance effects and were left in place between successive measurements. A PVC cover was machined to fit easily over the rings. To avoid pressure surges, the cover was carefully lowered over the ring prior to measuring soil gas fluxes. The chamber volume (ring plus cover) totaled 12 L. Gas was drawn through the chamber at a flow rate of 60–100 mL/min by a pump within the chemiluminescent detector. A separate stream of air (600–900 mL/min) was drawn through ascarite and drierite filters (to re-

move NO, CO₂, and H₂O) and mixed with the air flowing from the chamber to maintain the desired flow rate of 700–1000 mL/min at the detector. Stainless steel needle valves attached to mass flow meters (Sierra Instruments, model 821-1, Monterey, California, USA) were used to monitor and regulate flow through each pathway. Ambient air entered the chamber through inlet ports that had a combined area of 2.8 cm². Even small pressure changes caused by flow of air through chambers may cause errors in estimates of trace gas flux. To minimize this source of error, we used an inlet area to chamber volume ratio similar to that recommended by Denmead (1979).

Calibration of the detector with NO standards was performed in situ at the beginning and the end of the measurement period for each site. Tests for interfering gases (O₃, peroxyacetyl nitrate [PAN], CO₂) and for NO₂ showed that these gases were not detectable on any occasion, and that NO rather than NO₂ was the predominant form being measured. Davidson et al. (1991) and Williams and Davidson (1993) found similar results.

Nitric oxide fluxes were determined by measuring changes in NO concentrations in chambers for 8–12-min periods, depending on flux rates. Measurements were initiated one minute after the cover was placed on the ring. While NO concentrations were being measured, additional 30-mL gas samples were collected through a septum in the cover using a syringe. These samples were stored in evacuated tubes until they could be returned to the lab, where they were analyzed for N₂O and CO₂ using a Varian 3300 gas chromatograph (Varian, Walnut Creek, California, USA) equipped with electron capture and thermal-conductivity detectors. In all cases, however, N₂O fluxes were below detection limits ($<10\text{ ng N}_2\text{O-N}\cdot\text{m}^{-2}\cdot\text{s}^{-1}$). At the three New Mexico sites, N₂O and CO₂ production from separate forest floor and intact soil core samples was also measured during ¹⁵N isotopic dilution measurements. At the end of 24-h in situ isotopic dilution incubations, headspace gas was collected through septa in the lids of canning jars containing soil samples. These gas samples were also stored in evacuated tubes until they could be analyzed by gas chromatography for N₂O and CO₂.

After measuring ambient NO fluxes from each of the four to eight rings, one liter of distilled water was sprinkled over the soil surface inside each of the rings. This amount of water was equivalent to a 2-cm rainfall event. Water was added not only to see the effect of wetting on NO fluxes, but also to make soil moisture more similar to that created during gross N-cycling rate measurements (where ¹⁵N solutions were added). The containers of water were buried in the soil nearby before use, so that the water temperature would equilibrate with soil temperature. Immediately after water addition, the cover was replaced on the ring, and the flux was measured for ~10 min. The cover was then removed until another 10-min flux measurement was

initiated 55 min following addition of the water. Mean air temperatures and soil temperatures at 2 cm below the mineral soil surface were continuously recorded throughout the time NO fluxes were measured using thermistors and a 21X data logger (Campbell Scientific, Logan, Utah, USA).

Nitrogen-cycling rate measurements

At the five locations within each site, gross rates of N mineralization, nitrification, NH_4^+ consumption, and NO_3^- consumption were determined in forest floor material (O-horizon) and in intact 4.8-cm diameter by 15-cm deep mineral soil cores using $^{15}\text{NH}_4^+$ and $^{15}\text{NO}_3^-$ isotope dilution (Hart et al. 1994). Approximately 150 g fresh mass of forest floor material, consisting of all litter and organic debris above the mineral soil, was collected from the plots and placed in plastic bags. Twigs and branches >0.5 cm in diameter were removed, and the remaining material was broken up and homogenized by hand. A 5- to 10-g subsample was immediately extracted in 100 mL of 2-mol/L KCl solution for determination of initial NH_4^+ and NO_3^- concentrations. The remaining material was split, and 16 mL of a 30-mmol/L $^{15}\text{NH}_4^+$ solution (containing $[\text{NH}_4]_2\text{SO}_4$ at 99 atom percent ^{15}N) were added to one subsample, and 16 mL of a 30-mmol/L $^{15}\text{NO}_3^-$ solution (containing $\text{K}^{15}\text{NO}_3^-$ at 99 atom percent ^{15}N) were added to the other subsample. The ^{15}N solutions were added by dripping the solution onto the surface of the forest floor material and then mixing the sample thoroughly. Subsamples were immediately extracted in 2-mol/L KCl for determination of "time-zero" NH_4^+ and NO_3^- concentrations and ^{15}N enrichments. Additional subsamples were sealed in one-liter canning jars and reburied in the original plots. After 24 h of incubation in situ, the jars were excavated, a syringe was used to collect headspace gas samples (for N_2O and CO_2 concentrations), and the forest floor subsamples were extracted in 2-mol/L KCl for determination of final NH_4^+ and NO_3^- concentrations and ^{15}N enrichments. Gross inorganic N production and consumption rates ($\text{mg N}\cdot\text{kg}^{-1}\cdot\text{d}^{-1}$) were determined from changes in concentration and ^{15}N enrichment of NH_4^+ and NO_3^- pools during the 24-h incubation, using the equations of Kirkham and Bartholomew (1954). Net rates were calculated from the change in inorganic N concentrations during the incubation. All rates were converted from a mass basis to an areal basis ($\text{mg N}\cdot\text{m}^{-2}\cdot\text{d}^{-1}$) using the mean mass of forest floor material per unit area at each site. In some cases, it was not possible to calculate gross rates in forest floor material, because inorganic N concentrations at the end of the incubation were too low for ^{15}N analysis; however, it was still possible to calculate net rates for these samples.

Gross N-cycling rates were determined in intact mineral soil cores using ^{15}N isotope dilution and a concentric-core sampling technique (Davidson et al. 1991, Stark 2000). After removing forest floor material, poly-

carbonate cylinders (diameter, 4.8 cm; length, 15 cm) were pounded into the mineral soil. A second, larger diameter cylinder (diameter, 10 cm; length, 15 cm) was then driven into the soil to surround the smaller core. The core pair was excavated, and the soil trapped between the two cylinders was immediately homogenized and extracted in 2-mol/L KCl (~10:1 solution:soil mass ratio) to provide an estimate of initial NH_4^+ and NO_3^- concentrations in the inner soil core. The inner soil core was kept intact and injected with 16 mL of the same ^{15}N solutions used with the forest floor material. The ^{15}N solutions were injected into the soil cores using a syringe with a 15 cm long, 18-gauge side-port needle. First, the needle was inserted fully into the core, and then the syringe plunger was slowly depressed while the needle was being withdrawn. Eight 2-mL injections were made in each core to ensure that the solution was distributed uniformly throughout the entire soil core. A plastic cap was placed on the bottom of the soil core, the core was sealed in a one-liter canning jar, and the jar was reburied in the original plot for a 24-h in situ incubation. A second core pair was excavated and treated identically to the first core pair, except that the second inner core was extracted immediately (~10 min) after injection of the ^{15}N solution. This extract was used to determine what fraction of the added ^{15}N would have been recovered in the target pool (e.g., NH_4^+ or NO_3^-) at the beginning of the incubation. Time-zero pool sizes and ^{15}N enrichments in the intact incubated core were calculated based on the initial inorganic N concentrations measured in soil trapped between the inner and outer cores, the amount of ^{15}N added, and the ^{15}N recovery efficiency determined from the second core pair. At the end of the 24-h incubation, the jar containing the first soil core was excavated, a sample of the headspace was collected, and the soil was homogenized and extracted in 2-mol/L KCl to determine final inorganic N concentrations and ^{15}N enrichments. Within each plot, one set of cores was used for $^{15}\text{NH}_4^+$ isotope dilution measurements, and another set of cores was used for $^{15}\text{NO}_3^-$ isotope dilution measurements. Gross inorganic N production and consumption rates were determined using the equations described by Stark (2000). Gross N immobilization was calculated by subtracting net mineralization from gross mineralization. All rates were converted to an areal basis using the bulk density of <2 mm material in the 0–15-cm mineral soil layer measured at each plot.

All 2-mol/L KCl extracts were filtered and stored frozen until they could be analyzed. Concentrations of NH_4^+ and NO_3^- were determined colorimetrically using a Lachat flow-injection system (Lachat Instruments, Milwaukee, Wisconsin, USA). Extracts were prepared for ^{15}N analysis by a diffusion procedure (Stark and Hart 1996). The ^{15}N enrichments were determined by continuous-flow, direct-combustion, and isotope ratio mass spectrometry using a Europa Scientific ANCA 2020 system (PDZ, Cheshire, UK).

Soil characteristics

Gravimetric water contents of forest floor and mineral soil samples were determined by drying subsamples at 110°C for 36–48 h. Because water was added to the surface of the soil during NO flux measurements and the wetting front penetrated to varying depths, it was not possible to calculate water-filled pore space (WFPS) for these soils. Instead, WFPS was calculated for the intact mineral soil core samples based on the gravimetric water content after addition of the ¹⁵N solution, the soil bulk density, and the soil organic matter content. Bulk density was calculated based on the mass of oven-dry, <2-mm soil contained in the 271-cm³ polycarbonate cores used for isotope dilution measurements (after correcting for rock mass and volume). Mineral and organic fractions were assumed to have particle densities of 2.65 and 1.3 Mg/m³, respectively (Linn and Doran 1984). These estimates of WFPS represent relative differences among sites rather than the actual WFPS directly associated with the NO fluxes, because the method of water addition differed for NO flux and N-cycling rate measurements.

Total C and N were determined during direct-combustion and isotope ratio mass spectrometry of samples that had been dried at 70°C. Separate conversion factors were determined for each forest floor and mineral soil material for use in converting C and N concentrations to an oven-dry (110°C) basis. Soil pH was measured in 0.01 mol/L CaCl₂ (2:1 solution : soil mass ratio; Hendershot et al. 1993).

Nitrification potential assays of forest floor and mineral soil were performed in the laboratory using the shaken soil slurry method (Hart et al. 1994). Approximately 10–15 g moist soil or forest floor material were continuously shaken with 100 mL of a dilute phosphate buffer containing 0.5 mmol/L (NH₄)₂SO₄. The nitrification potential rate was equal to the rate of NO₃⁻ accumulation during a 24-h incubation.

Statistical analyses

Prior to statistical analyses, all variables were tested for normal distributions using the Anderson-Darling test provided in the Minitab statistical software (Release 11.21; Minitab, State College, Pennsylvania, USA). All variables not showing normal distributions ($P < 0.05$) were successfully normalized by log₁₀-transformation. Ambient NO fluxes, and fluxes five minutes and one hour after water addition were regressed against 34 soil and forest floor variables to (1) test whether gross rates of nitrification were correlated with NO fluxes; and (2) determine which soil characteristics were good predictors of NO fluxes. Because we lacked a priori hypotheses on relationships, linear regression models were always used with the transformed data. However, back-transformation of independent variables prior to graphing made several of the relationships nonlinear.

Many of the independent variables were correlated. Multicollinearity among the independent variables makes it difficult to sort out cause-and-effect relationships between the individual soil variables and NO fluxes. In addition, there are too many independent variables (34), relative to the number of sites where NO flux measurements were carried out (9), for valid use of multiple regression to determine which of the independent variables are the best predictors of NO flux. Therefore, a principal-components analysis (PCA) was used to reduce the number of variables to a few uncorrelated composite variables (principal components) representing C- and N-cycling trends across the nine sites. The first three principal components were then regressed vs. NO fluxes to test their ability to predict NO flux. All statistical analyses were performed using Minitab statistical software.

RESULTS

Ambient soil NO fluxes from the nine sites ranged from a low of 0.02 ng NO-N·m⁻²·s⁻¹ at the western hemlock–sitka spruce forest on the Oregon coast to highs of 0.58 ng·m⁻²·s⁻¹ at the aspen forest in New Mexico and 1.11 ng·m⁻²·s⁻¹ at the sagebrush–steppe site in northern Utah (Table 1). Addition of 2 cm of water caused an immediate increase in NO fluxes at almost all of the sites. Fluxes increased by 12–2200% during the 10 min immediately following wetting, except at the Oregon hemlock–spruce forest, where rates did not change, and at the New Mexico aspen forest, where rates declined by 61%. One hour after wetting, the elevated fluxes were either sustained or increased even further, except at the Oregon ponderosa pine and mountain hemlock–silver fir sites where they returned to near ambient rates. Fluxes five minutes and one hour after wetting were highly correlated ($\text{flux}_{1\text{h}} = -0.03 + 0.70\text{flux}_{5\text{min}} + 0.32(\text{flux}_{5\text{min}})^2$; $r = 0.89$; $P = 0.009$); however, neither was correlated with the ambient rate ($P > 0.05$).

Nitric oxide fluxes measured before water addition (ambient fluxes) were not correlated with any of the gross or net rate measurements (Table 2). Ambient fluxes were positively correlated with pH and bulk density, and negatively correlated with soil organic carbon (SOC), clay content, ambient soil wetness, and post-wetting water-filled pore space (WFPS). These relationships were strongly influenced by the low ambient fluxes measured at the Oregon hemlock–spruce and mountain hemlock sites (Fig. 2a–d), with the exception of the relationship between NO flux and pH. These independent variables were also highly intercorrelated: Sites with higher pH (and higher NO fluxes) tended to have higher bulk density, lower initial water contents, lower WFPS following wetting, and less soil organic matter.

Nitric oxide fluxes following wetting were not correlated with gross nitrification rates in either the mineral soil or the forest floor material (Table 2; Fig. 3a,

TABLE 2. Pearson correlation coefficients for mineral soil and forest floor (ff) characteristics vs. NO flux rates ($\text{ng N}\cdot\text{m}^{-2}\cdot\text{s}^{-1}$).

Independent variable	Units	Data transformation†	NO flux‡		
			Ambient	5 min	1 h
Gross rates					
	$\text{mg N}\cdot\text{m}^{-2}\cdot\text{d}^{-1}$				
Mineralization (soil)		$\log(x)$	0.181	0.345	0.579
Mineralization (ff; 8)§			0.016	0.166	0.098
Nitrification (soil)			0.014	0.080	0.002
Nitrification (ff; 6)§			-0.547	-0.603	-0.523
N immobilization (soil)			0.094	-0.518	-0.329
N immobilization (ff; 8)§			0.315	-0.135	-0.165
NH_4^+ consumption (soil)			-0.116	-0.567	-0.361
NH_4^+ consumption (ff; 8)§		$\log(x)$	0.172	-0.245	-0.481
NO_3^- consumption (soil)		$\log(x)$	0.034	-0.108	-0.314
NO_3^- consumption (ff; 8)§			-0.378	-0.813*	-0.870**
Net rates					
	$\text{mg N}\cdot\text{m}^{-2}\cdot\text{d}^{-1}$				
Mineralization (soil)		$\log(x + 70)$	0.537	0.745*	0.857**
Mineralization (ff)			-0.263	0.315	0.331
Ammonification (soil)		$\log(x + 130)$	0.657	0.820*	0.824*
Ammonification (ff)			-0.338	0.271	0.320
Nitrification (soil)			0.008	0.141	0.547
Nitrification (ff)			0.349	0.402	0.756*
Potential nitrification (soil)	$\text{mg N}\cdot\text{m}^{-2}\cdot\text{d}^{-1}$	$\log(x)$	0.207	0.239	0.560
Potential nitrification (ff)	$\text{mg N}\cdot\text{m}^{-2}\cdot\text{d}^{-1}$		-0.086	-0.184	-0.042
KCl-extractable N					
	$\text{mg N}/\text{m}^2$				
NH_4^+ (soil)			0.391	-0.301	-0.096
NH_4^+ (ff)		$\log(x)$	-0.049	-0.184	-0.368
NO_3^- (soil)			0.552	0.694*	0.812*
NO_3^- (ff)			-0.228	-0.175	0.125
Mineral soil					
Soil organic carbon	$\text{kg SOC}/\text{kg soil}$	$\log(x)$	-0.761*	-0.732*	-0.862**
C:N	$\text{kg C}/\text{kg N}$		-0.348	-0.330	-0.670*
Ambient wetness	$\text{kg H}_2\text{O}/\text{kg soil}$	$\log(x)$	-0.821*	-0.779*	-0.855**
Water-filled pore space	$\text{m}^3/\text{m}^3 \text{ soil}$		-0.715*	-0.823*	-0.711*
Temperature	$^{\circ}\text{C}$		0.437	0.436	0.623
pH	...		0.867**	0.728*	0.713*
Bulk density	Mg/m^3		0.848**	0.800*	0.922**
Sand	$\text{kg sand}/\text{kg soil}$		0.647	0.509	0.223
Clay	$\text{kg clay}/\text{kg soil}$		-0.684*	-0.537	-0.224
Forest floor mass	kg/m^2	$\log(x)$	-0.341	-0.242	-0.618
Forest floor C:N	$\text{kg C}/\text{kg N}$		-0.267	-0.208	-0.271
Principal components					
PC-1			0.544	0.666*	0.894**
PC-2			-0.578	-0.599	-0.310
PC-3			0.423	-0.176	-0.060

* $P < 0.05$; ** $P < 0.005$.

† Prior to regression, data were transformed as indicated to obtain normal distributions and equal variances. If no transformation is indicated, data remained untransformed.

‡ Dependent variable was NO flux either before addition of water (ambient), or five minutes or one hour after water addition. All NO flux data were \log transformed.

§ $N = 9$ for all variables except where a number indicates otherwise ($N = 6$ or 8).

b). The only gross rate that was correlated with NO fluxes either five minutes or one hour after water addition was NO_3^- consumption in the forest floor. Sites with faster gross rates of NO_3^- consumption had lower NO fluxes (Fig. 3d).

In contrast to gross rates, net rates were significantly correlated with NO fluxes following wetting. Net N mineralization and ammonification rates in the mineral soil and net nitrification rates in the forest floor were all positively correlated with fluxes five minutes and one hour after wetting (Table 2; Fig. 3c, e, f). While the relationships between NO flux and both net mineralization and net ammonification appear to be strong-

ly influenced by data from the Douglas-fir site, elimination of this site actually improved the fit (net mineralization, $r^2 = 0.83$, $P = 0.002$; net ammonification, $r^2 = 0.69$, $P = 0.008$). Nitric oxide fluxes following wetting were positively correlated with soil NO_3^- content, pH, and bulk density, but they were negatively correlated with SOC, soil C:N, ambient wetness, and WFPS (Table 2, Fig. 4a-f).

Principal-component analysis identified three composite variables that explained 75% of the variance in soil characteristics across the nine sites (Table 3). The first principal component (PC-1), which explained 37% of the variance, represented a composite variable that

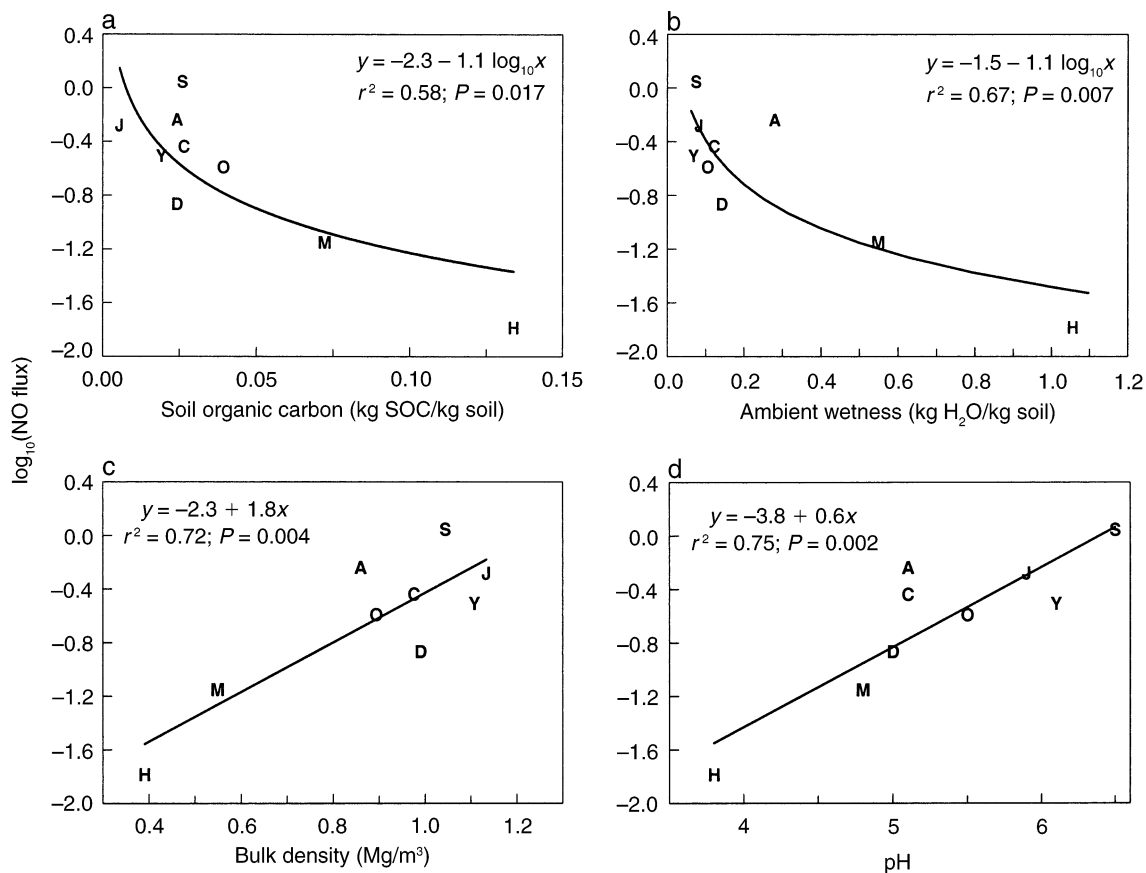


FIG. 2. Relationships between \log -transformed values of ambient NO fluxes (original data in $\text{ng N}\cdot\text{m}^{-2}\cdot\text{s}^{-1}$) and various mineral soil characteristics. Curvilinear regression lines are the result of back-transformation of independent variables prior to plotting. See Table 1 for key to letter symbols.

was strongly influenced by net N mineralization rates, especially when they corresponded with high net nitrification rates and soil NO_3^- contents. For example, net mineralization, net ammonification, net nitrification, and soil NO_3^- all had highly positive loading rates in PC-1. Variables normally expected to be negatively correlated with net N mineralization, such as soil C:N, SOC, and forest floor mass all had highly negative loading rates in PC-1 (Fig. 5). Other soil variables with high positive loading rates in PC-1 were either positively correlated with net mineralization or negatively correlated with SOC. For example, gross N mineralization in mineral soil is positively correlated with net mineralization ($r = 0.80$), net ammonification ($r = 0.68$), and net nitrification rates ($r = 0.80$); nitrification potential is positively correlated with net nitrification ($r = 0.90$); and pH and bulk density are negatively correlated with SOC ($r = -0.71$ and -0.89 , respectively).

The second (PC-2) and third (PC-3) principal components explained 23% and 15% of the variance in soil characteristics, respectively. The axis PC-2 represents somewhat of a textural gradient, with large positive loadings for clay and WFPS, and a large negative load-

ing for sand; however, forest floor NO_3^- content also had a large negative loading (Table 3). The axis PC-3 had large positive loadings for gross N immobilization, gross NH_4^+ consumption, and soil NH_4^+ contents, and a large negative loading for net ammonification in the forest floor. This axis appears to represent a continuum of sites where high soil NH_4^+ concentrations were associated with high rates of NH_4^+ assimilation, but not nitrification.

Nitric oxide fluxes measured prior to water addition were not correlated with any of the three principal components. In contrast, NO fluxes after wetting were positively correlated with the first principal component (fluxes five minutes after wetting, $r = 0.67$, $P < 0.05$; fluxes one hour after wetting, $r = 0.89$, $P < 0.001$; Table 2, Fig. 6).

DISCUSSION

Our primary objective was to identify which soil characteristics are most important in regulating NO fluxes from forest and rangeland soils. In previous surveys of diverse ecosystems, NO fluxes were found to be positively correlated with net N-cycling rates and accumulation of NO_3^- (Williams and Fehsenfeld 1991,

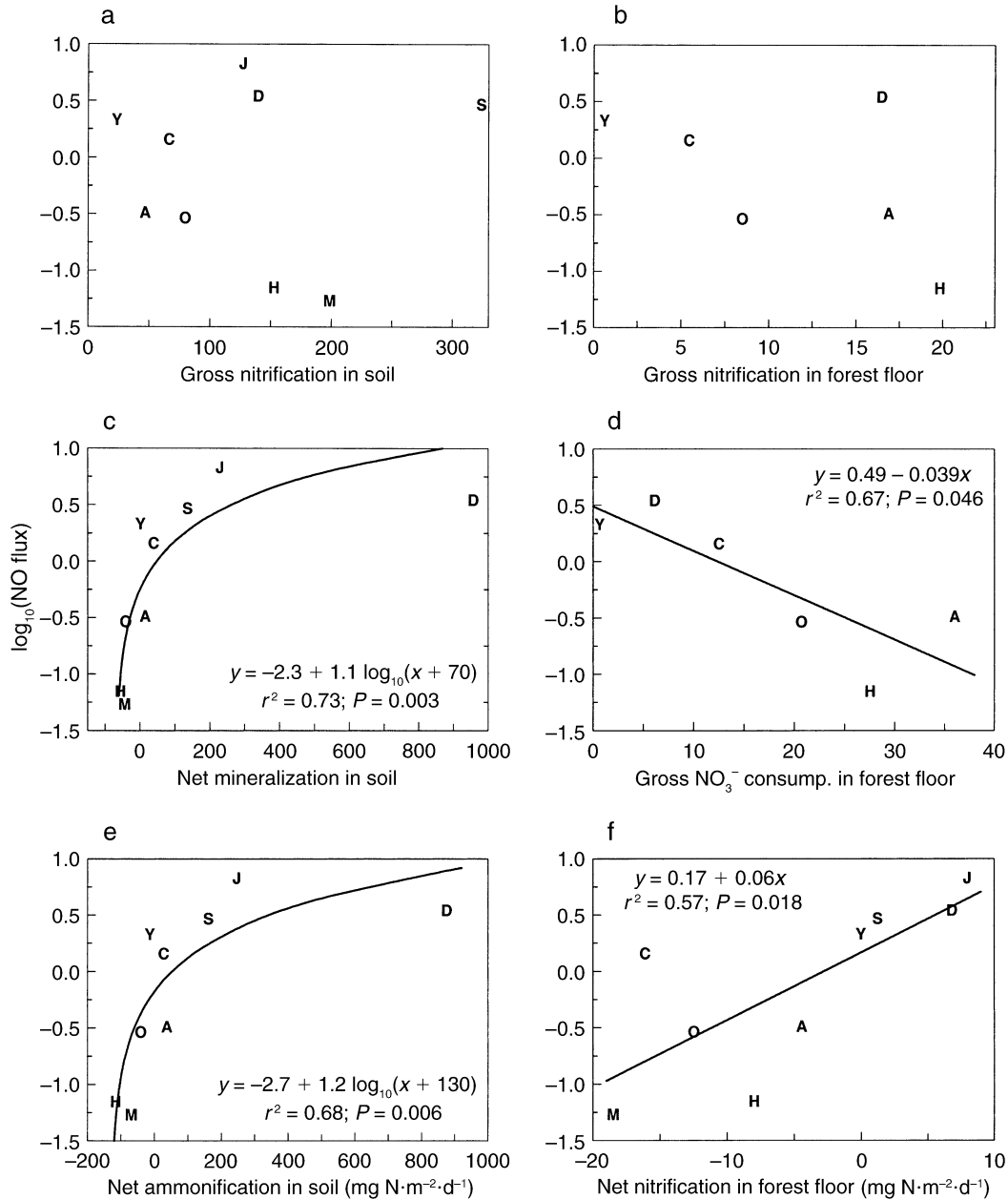


FIG. 3. Relationships between log-transformed values of NO fluxes (original data in $\text{ng N}\cdot\text{m}^{-2}\cdot\text{s}^{-1}$) one hour after addition of water and various gross and net N-cycling rates in the mineral soil and forest floor. Curvilinear regression lines are the result of back-transformation of independent variables prior to plotting. See Table 1 for key to letter symbols.

Davidson and Schimel 1995, Serca et al. 1998, Verchot et al. 1999, Hartley and Schlesinger 2000). It has been frequently assumed that higher net rates indicate higher gross nitrification rates, and thus, that NO fluxes are largely regulated by gross rates. Our study, which is the first to measure gross nitrification rates along with NO fluxes at a wide variety of sites, shows that this conclusion is incorrect. We did find that NO fluxes were correlated with net N-cycling rates, but they were not

correlated with either gross nitrification or gross N mineralization.

Although NO fluxes were uncorrelated with gross nitrification rates, our results do provide evidence that the primary source of NO was nitrification, rather than denitrification or chemodenitrification. First, NO fluxes following wetting were negatively correlated with gross rates of NO_3^- consumption, rather than positively correlated as would be expected if denitrification were

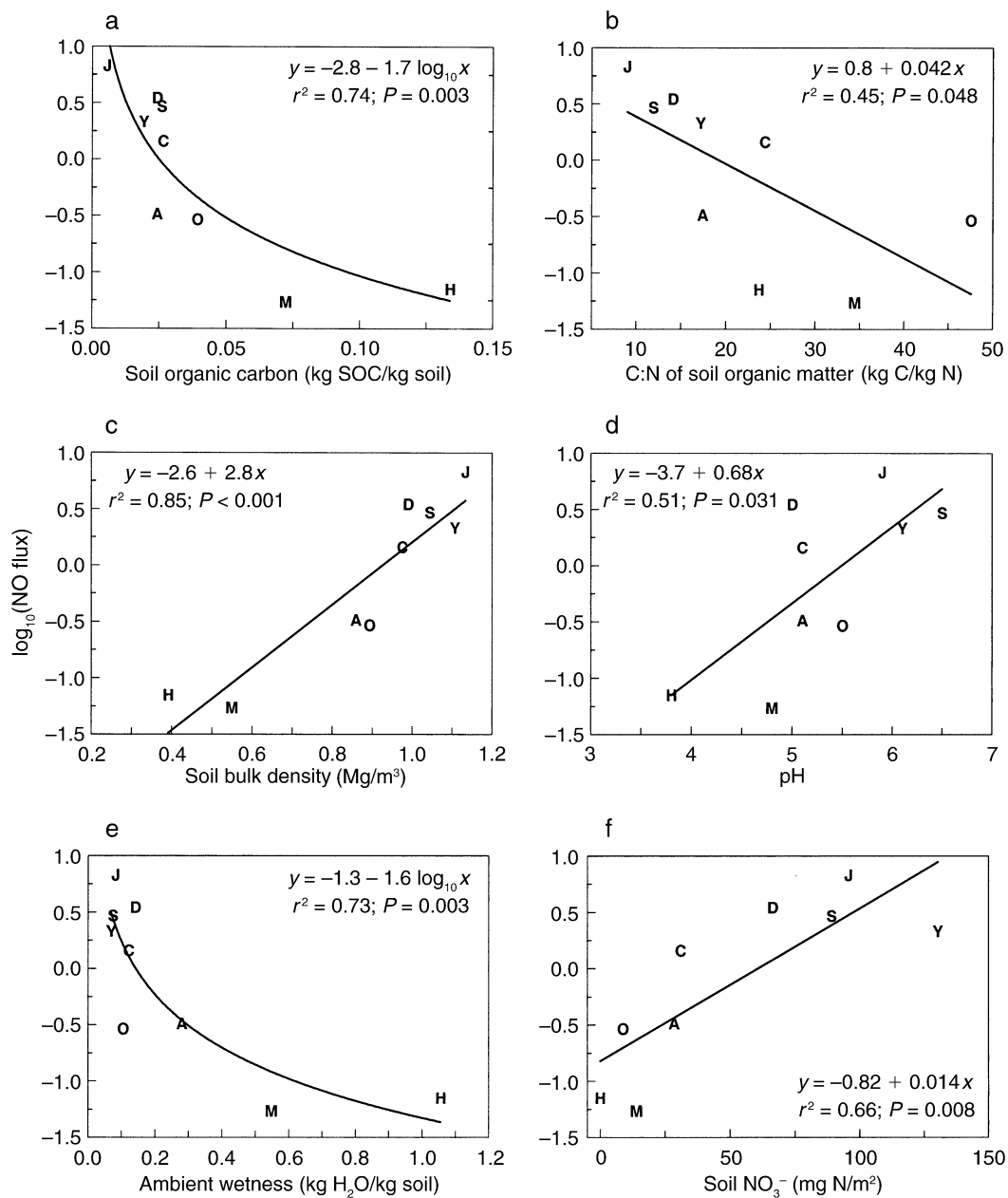


FIG. 4. Relationships between \log -transformed values of NO fluxes (original data in $\text{ng N}\cdot\text{m}^{-2}\cdot\text{s}^{-1}$) one hour after addition of water and various mineral soil characteristics. Curvilinear regression lines are the result of back-transformation of independent variables prior to plotting. See Table 1 for key to letter symbols.

occurring. Second, at all sites, N₂O fluxes in the chambers were below detection limits, both before and after wetting. At the three New Mexico sites, we measured N₂O accumulation in canning jars containing the forest floor material and soil cores, as well as in the chambers. By converting N₂O production in the jars to an areal basis and summing N₂O production from forest floor material and mineral soil, we calculate that N₂O:NO

ratios were ~ 0.39 at the aspen forest, ~ 0.12 at the mixed conifer forest, and ~ 0.007 at the pinyon–juniper woodland. Such low ratios of N₂O:NO production suggest that nitrification was the predominant NO source, rather than denitrification (Firestone and Davidson 1989).

Our results also indicate that chemodenitrification was not an important source of NO. Chemodenitrifi-

TABLE 3. Results of principal-component analysis (PCA) showing loading rates of soil variables for the first three principal components.

Soil variable	PC-1	PC-2	PC-3
Eigenvalue	10.32	6.38	4.28
Cumulative proportion of variance explained	0.37	0.60	0.75
Gross rates			
Mineralization (soil)	0.232*	0.172	-0.090
Nitrification (soil)	0.078	0.140	-0.046
Immobilization (soil)	-0.057	0.168	0.417**
NH ₄ ⁺ consumption (soil)	-0.046	0.245	0.361*
NO ₃ ⁻ consumption (soil)	-0.049	0.044	0.120
Net rates			
Mineralization (soil)	0.259*	-0.053	-0.161
Mineralization (ff)	0.186	0.212	-0.225
Ammonification (soil)	0.239*	-0.133	-0.132
Ammonification (ff)	0.149	0.118	-0.366*
Nitrification (soil)	0.219*	0.208	-0.164
Nitrification (ff)	0.286**	0.078	0.003
Potential nitrification (soil)	0.243*	0.140	-0.090
Potential nitrification (ff)	-0.094	-0.074	-0.222
KCl-extractable N			
NH ₄ ⁺ (soil)	0.037	0.116	0.324*
NH ₄ ⁺ (ff)	-0.211*	-0.163	-0.111
NO ₃ ⁻ (soil)	0.272**	-0.057	0.121
NO ₃ ⁻ (ff)	-0.063	-0.290*	-0.198
Mineral soil			
Organic carbon	-0.228*	0.186	-0.086
C:N	-0.245*	-0.162	-0.089
Ambient wetness	-0.213*	0.270	-0.047
Water-filled pore space	-0.187	0.289*	0.005
Temperature	0.247*	-0.019	0.118
pH	0.212*	-0.218	0.184
Bulk density	0.237*	-0.234	0.055
Sand	0.025	-0.320*	0.215
Clay	-0.002	0.359**	-0.148
Forest floor mass	-0.256*	-0.109	-0.178
Forest floor C:N	-0.093	-0.127	-0.137

Notes: Soil variables were included in PCA only when data were available for all sites ($N = 9$). Data were transformed as indicated in Table 2.

* $P < 0.05$; ** $P < 0.005$; significance level of loading rates.

cation occurs at low pH when nitrite either autodecomposes or reacts with soil organic matter to form NO (Nelson 1982, Blackmer and Cerrato 1986); however, in our study soil materials that had high pH (and low organic matter) had the greatest NO flux (Fig. 4d). Furthermore, intensive experiments at the sagebrush-steppe site showed that addition of NH₄⁺ during wetting stimulated NO flux, but addition of either sucrose or NO₃⁻ had no effect on NO fluxes (Smart et al. 1999). All of these results are consistent with previous studies showing that nitrification is the predominant source of NO emissions from soils of temperate ecosystems (Anderson et al. 1988, Skiba et al. 1992, Smart et al. 1999).

The lack of correlation between gross nitrification rates and NO flux indicates that the "flow through the pipe" is not the primary regulator of NO emissions. Our study included several coniferous forests with low pH, low NH₄⁺ availability, and often, undetectable NO₃⁻ concentrations. These are ecosystems that would be expected to have extremely low nitrification rates. However, even at the sites with the lowest nitrification

rates, gross nitrification rates were still >100-fold higher than ambient and postwetting NO fluxes. Because NO flux represents such a small fraction of the total product, even the lowest nitrification rates could decline further without limiting NO flux.

The few other studies that measured both gross nitrification rates and NO fluxes also failed to show significant positive relationships between NO fluxes and gross rates. In a laboratory study examining three agricultural soils, Venterea and Rolston (2000) found no correlation between NO fluxes and gross nitrification. Mean NO fluxes and gross nitrification rates reported by Davidson et al. (1993b) for four grazed and ungrazed plots in an oak woodland-annual grassland were not significantly correlated ($P = 0.16$). Although Davidson et al. (1993a) concluded that NO flux and N-transformation rates were related at their two study sites, their data show that the site with the highest NO flux actually had the lowest gross nitrification rate.

While post-wetting NO flux was uncorrelated with gross nitrification rate, it was strongly correlated with

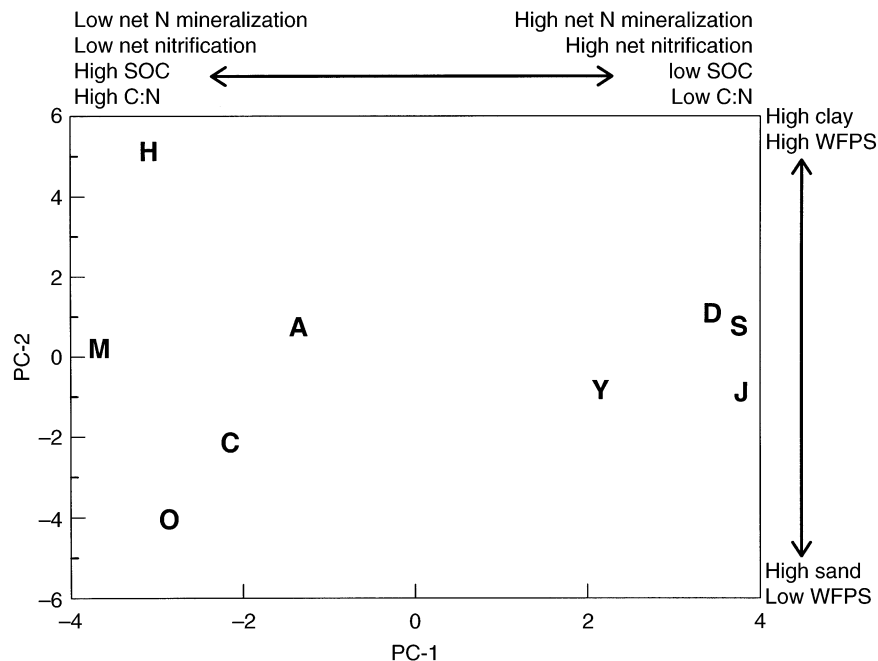


FIG. 5. Separation of study sites based on the first two principal components. See Table 1 for key to letter symbols. Trends are indicated along the top and right sides of the figure.

net mineralization, net ammonification, net nitrification, soil NO_3^- , pH, and bulk density (Table 2). Nitric oxide flux was negatively correlated with gross NO_3^- consumption in the forest floor, soil organic carbon (SOC), and soil C:N ratio. The principal-components

analysis (PCA) showed that these soil variables were intercorrelated and that NO fluxes increased along a gradient of increasing net N mineralization and nitrification, and decreasing soil C availability and C:N ratio.

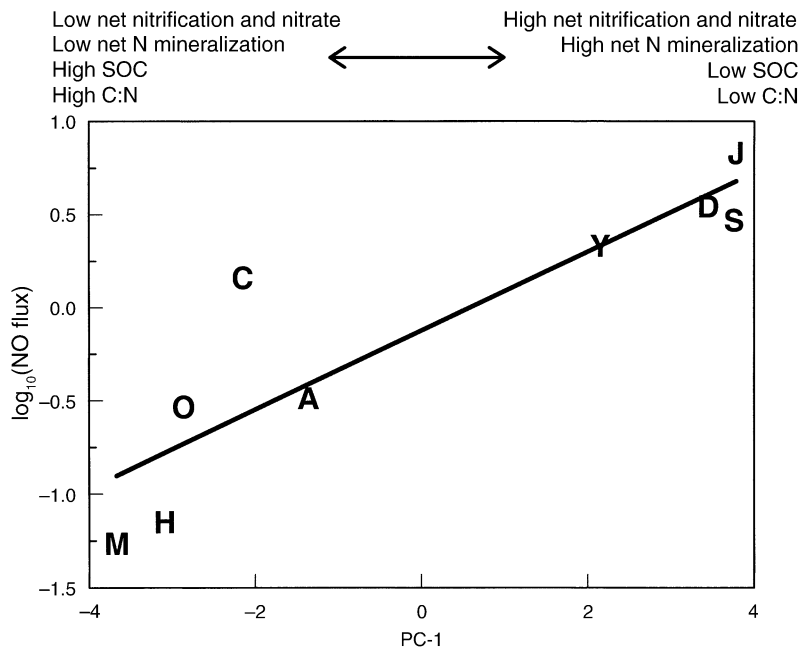


FIG. 6. Relationship between \log_{10} -transformed values of NO fluxes (original data in $\text{ng N}\cdot\text{m}^{-2}\cdot\text{s}^{-1}$) one hour after addition of water and the first principal component ($r^2 = 0.80$, $P < 0.001$). See Table 1 for key to letter symbols. Trends are indicated along the top of the figure.

These results, showing that NO fluxes were correlated with net rates, but not gross rates, indicate that the balance between inorganic N production and consumption is more important in regulating NO flux than production processes alone. Low net rates of mineralization and nitrification occur in soils where microorganisms have high assimilatory demands for inorganic N relative to the supply. In these soils, as NO diffuses away from the microsite where it was produced, it is more likely to be consumed by microorganisms in other microsites where assimilatory demands for N are high. As a result, less NO reaches the soil surface. Conversely, in soils where gross N mineralization exceeds the assimilatory demands of microbes, net rates are high, less NO is consumed, and more NO reaches the soil surface. Our results, showing that high gross rates of NO_3^- consumption in the forest floor were associated with lower NO fluxes, supports this explanation. Also, our observation that soils with high SOC and C:N ratios had lower NO flux is consistent with this interpretation, because high SOC and C:N ratios indicate higher C availability to microbes, greater assimilatory demand for N relative to N supply, and more NO assimilation. Finally, our explanation is consistent with results from other studies showing that long-term fertilization or N deposition, which saturates the microbial demand for N, increases trace N gas flux (Slemr and Seiler 1984, Fenn et al. 1996, Martin et al. 1998, Hall and Matson 1999).

Soils exposed to high NO concentrations, such as those associated with polluted air, have been shown to act as NO sinks (Johansson and Galbally 1984, Slemr and Seiler 1984, Baumgartner and Conrad 1992, Skiba et al. 1994). Some of this NO consumption results from abiotic oxidation and dissolution of NO in soil solution forming NO_2^- and NO_3^- (Stark and Firestone 1995); however, NO oxidation by heterotrophic microorganisms has also been identified as an important consumptive fate for NO in soils receiving organic C additions (Baumgartner et al. 1996, Dunfield and Knowles 1997). Dunfield and Knowles (1998) concluded that NO consumption was a function of heterotrophic microbial activity; thus, CO_2 flux and soil organic matter contents should be good predictors of net NO uptake by soils exposed to high NO concentrations. While we found that SOC concentrations were negatively correlated with NO flux (Table 2), CO_2 flux rates were not significantly correlated with either ambient NO flux rates ($r = -0.42$, $P = 0.26$), or fluxes after five minutes ($r = 0.14$, $P = 0.72$) or one hour ($r = 0.19$, $P = 0.61$). These results suggest that it is not heterotrophic microbial activity per se, but the assimilatory demand for N relative to the supply rate that controls the balance between NO production and consumption. Net rates of N mineralization and nitrification appear to be good predictors of this balance, even across a wide range of forest and rangeland ecosystems.

These results suggest that certain aspects of global

change may have substantial impacts on soil NO flux. Hall and Matson (1999) recently proposed that increased rates of atmospheric N deposition are likely to increase soil NO flux, especially in tropical systems. Our results support this perspective; however, they also indicate that changes in C availability may be of equal importance in determining the response of NO fluxes to global change. For example, if elevated temperatures result in a decline in SOC pools, increases in NO flux may be accentuated. Conversely, if elevated atmospheric CO_2 results in greater net primary production or addition of higher C:N organic matter to soils, increases in NO flux resulting from N deposition may be diminished.

Hutchinson et al. (1997) concluded that the greatest limitation to current coarse-scale models predicting NO emissions is their failure to account for the large pulse of NO following wetting of dry soil. We found that net mineralization and net nitrification rates were strongly related to the magnitude of the NO pulse following wet-up. Therefore, net N-cycling rates, rather than gross rates, are likely to be better predictors of annual NO fluxes from soils. This information should aid efforts to model soil NO emissions, because net N-cycling rates are more easily measured than gross N-cycling rates, and extensive data sets on net rates already exist for many forest, rangeland, and agricultural soils.

ACKNOWLEDGMENTS

We thank G. Mileski, Y. Myint, E. Smith, J. Hart, R. Wright, P. Roosma, M. Swarts, and V. Diego for assistance with field and laboratory work; C. Glassman for providing additional laboratory facilities, and S. Durham and P. Saetre for statistical advice. This work was supported by grants from the National Science Foundation Division of Ecosystem Studies (9208828 and 9807097), U.S. Department of Agriculture Cooperative State Research Service (USDA-CSRS) (92-37101-7976), and the Utah Agricultural Experiment Station, Logan, Utah, USA.

LITERATURE CITED

- Anderson, I. C., J. S. Levine, M. A. Poth, and P. J. Riggan. 1988. Enhanced biogenic emissions of nitric oxide and nitrous oxide following surface biomass burning. *Journal of Geophysical Research* **93**:3893–3898.
- Baumgartner, M., and R. Conrad. 1992. Effect of soil variables and season on the production and consumption of nitric oxide in oxic soils. *Biology and Fertility of Soils* **14**:166–174.
- Baumgartner, M., M. Koschorreck, and R. Conrad. 1996. Oxidative consumption of nitric oxide by heterotrophic bacteria in soil. *Federation of European Microbiological Societies (FEMS) Microbial Ecology* **19**:165–170.
- Blackmer, A. M., and M. E. Cerrato. 1986. Soil properties affecting formation of nitric oxide by chemical reactions of nitrite. *Soil Science Society of America Journal* **50**:1215–1218.
- Bollmann, A., and R. Conrad. 1998. Influence of O_2 availability on NO and N_2O release by nitrification and denitrification in soils. *Global Change Biology* **4**:387–396.
- Conrad, R. 1996. Soil microorganisms as controllers of atmospheric trace gases (H_2 , CO, CH_4 , OCS, N_2O , and NO). *Microbiological Reviews* **60**:609–640.
- Davidson, E. A. 1991. Fluxes of nitrous oxide and nitric

- oxide from terrestrial ecosystems. Pages 219–235 in J. E. Rogers and W. B. Whitman, editors. Microbial production and consumption of greenhouse gases: methane, nitrogen oxides, and halomethanes. American Society for Microbiology, Washington, D.C., USA.
- Davidson, E. A., S. C. Hart, C. A. Shanks, and M. K. Firestone. 1991. Measuring gross nitrogen mineralization, immobilization, and nitrification by ^{15}N isotope dilution in intact soil cores. *Journal of Soil Science* **42**:335–349.
- Davidson, E. A., D. H. Herman, A. Schuster, and M. K. Firestone. 1993b. Cattle grazing and oak trees as factors affecting soil emissions of nitric oxide from an annual grassland. Pages 109–120 in D. E. Rolston, editor. Agricultural ecosystem effects on trace gases and global climate change. Agronomy Society of America, Madison, Wisconsin, USA.
- Davidson, E. A., M. Keller, H. E. Erickson, L. V. Verchot, and E. Veldkamp. 2000. Testing a conceptual model of soil emissions of nitrous and nitric oxides. *BioScience* **50**:667–680.
- Davidson, E. A., and W. Kinglerlee. 1997. A global inventory of nitric oxide emissions from soils. *Nutrient Cycling in Agroecosystems* **48**:37–50.
- Davidson, E. A., P. A. Matson, P. M. Vitousek, R. Riley, K. Duncan, G. Garcia-Mendez, and J. M. Maass. 1993a. Processes regulating soil emissions of NO and N_2O in a seasonally dry tropical forest. *Ecology* **74**:130–139.
- Davidson, E. A., and J. P. Schimel. 1995. Microbial processes of production and consumption of nitric oxide, nitrous oxide and methane. Pages 327–357 in P. A. Matson and R. C. Harriss, editors. Biogenic trace gases: measuring emissions from soil and water. Blackwell, Cambridge, Massachusetts, USA.
- Davidson, E. A., P. M. Vitousek, P. A. Matson, R. Riley, G. Garcia-Mendez, and J. M. Maass. 1991. Soil emissions of nitric oxide in a seasonally dry tropical forest of Mexico. *Journal of Geophysical Research* **96**:15439–15445.
- Denmead, O. T. 1979. Chamber systems for measuring nitrous oxide emissions from soils in the field. *Soil Science Society of America Journal* **43**:89–95.
- Dunfield, P. F., and R. Knowles. 1997. Biological oxidation of nitric oxide in a humisol. *Biology and Fertility of Soils* **24**:294–300.
- Dunfield, P. F., and R. Knowles. 1998. Organic matter, heterotrophic activity, and NO consumption in soils. *Global Change Biology* **4**:199–207.
- Fenn, M. E., M. A. Poth, and D. A. Johnson. 1996. Evidence for nitrogen saturation in the San Bernardino Mountains in southern California. *Forest Ecology and Management* **82**:211–230.
- Firestone, M. K., and E. A. Davidson. 1989. Microbiological basis of NO and N_2O production and consumption in soil. Pages 7–21 in M. O. Andreae and D. S. Schimel, editors. Exchange of trace gases between terrestrial ecosystems and the atmosphere. John Wiley and Sons, New York, New York, USA.
- Gholz, H. L. 1982. Environmental limits on aboveground net primary production, leaf area, and biomass in vegetation zones of the Pacific Northwest. *Ecology* **63**:469–481.
- Godde, M., and R. Conrad. 1998. Simultaneous measurement of nitric oxide production and consumption in soil using a simple static incubation system, and the effect of soil water content on the contribution of nitrification. *Soil Biology and Biochemistry* **30**:433–442.
- Gosz, J. R. 1980. Nutrient budget studies for forests along an elevational gradient in New Mexico. *Ecology* **61**:515–521.
- Hall, S. J., and P. A. Matson. 1999. Nitrogen oxide emissions after nitrogen additions in tropical forests. *Nature* **400**:152–155.
- Hart, S. C., J. M. Stark, E. A. Davidson, and M. K. Firestone. 1994. Mineralization, immobilization, and nitrification. Pages 985–1018 in R. Weaver, editor. Methods of soil analysis. Soil Science Society of America, Madison, Wisconsin, USA.
- Hartley, A. E., and W. H. Schlesinger. 2000. Environmental controls on nitric oxide emission from northern Chihuahuan desert soils. *Biogeochemistry* **50**:279–300.
- Hendershot, W. H., H. Lalonde, and M. Duquette. 1993. Soil reactions and exchangeable acidity. Pages 141–145 in M. R. Carter, editor. Soil sampling and methods of analysis. CRC Press, Boca Raton, Florida, USA.
- Hutchinson, G. L., M. F. Vigil, J. W. Doran, and A. Kessavalou. 1997. Coarse-scale soil-atmosphere NO_x exchange modeling: status and limitations. *Nutrient Cycling in Agroecosystems* **48**:25–35.
- Johansson, C., and I. E. Galbally. 1984. Production of nitric oxide in loam under aerobic and anaerobic conditions. *Applied and Environmental Microbiology* **47**:1284–1289.
- Kirkham, D., and W. V. Bartholomew. 1954. Equations for following nutrient transformations in soil, utilizing tracer data. *Soil Science Society of America Proceedings* **18**:33–34.
- Linn, D. M., and J. W. Doran. 1984. Effect of water-filled pore space on carbon dioxide and nitrous oxide production in tilled and nontilled soils. *Soil Science Society of America Journal* **48**:1267–1272.
- Logan, J. 1983. Nitrogen oxides in the troposphere: global and regional budgets. *Journal of Geophysical Research* **88**:10785–10807.
- Martin, R. E., M. C. Scholes, A. R. Mosier, D. S. Ojima, E. A. Holland, and W. J. Parton. 1998. Controls on annual emissions of nitric oxide from soils of the Colorado short-grass steppe. *Global Biogeochemical Cycles* **12**:81–91.
- Matson, P. 1997. NO_x emission from soils and its consequences for the atmosphere and biosphere: critical gaps and research directions for the future. *Nutrient Cycling in Agroecosystems* **48**:1–6.
- Matson, P. A., and P. M. Vitousek. 1987. Cross-system comparisons of soil nitrogen transformations and nitrous oxide flux in tropical forest ecosystems. *Global Biogeochemical Cycles* **1**:163–170.
- Nelson, D. W. 1982. Gaseous losses of nitrogen other than through denitrification. Pages 327–364 in F. J. Stevenson, editor. Nitrogen in agricultural soils. American Society of Agronomy, Madison, Wisconsin, USA.
- Otter, L. B., W. X. Yang, M. C. Scholes, and F. X. Meixner. 1999. Nitric oxide emissions from a southern African savanna. *Journal of Geophysical Research* **104**(D15):18471–18485.
- Papen, H., R. von Berg, I. Hinkel, B. Thoene, and H. Renneberg. 1989. Heterotrophic nitrification by *Alcaligenes faecalis*: NO_2^- , NO_3^- , N_2O , and NO production in exponentially growing cultures. *Applications of Environmental Microbiology* **55**:2068–2072.
- Parton, W. J., E. A. Holland, S. J. Del Grosso, M. D. Hartman, R. E. Martin, A. R. Mosier, D. S. Ojima, and D. S. Schimel. 2001. Generalized model for NO_x and N_2O emissions from soils. *Journal of Geophysical Research* **106**(D15):17403–17419.
- Potter, C. S., P. A. Matson, P. M. Vitousek, and E. A. Davidson. 1996. Process modeling of controls on nitrogen trace gas emissions from soils worldwide. *Journal of Geophysical Research* **101**:1361–1377.
- Potter, C. S., R. H. Riley, and S. A. Klooster. 1997. Simulation modeling of nitrogen trace gas emissions along an age gradient of tropical forest soils. *Ecological Modeling* **97**:179–196.
- Riley, R. H., and P. M. Vitousek, P. M. 1995. Nutrient dynamics and nitrogen trace gas flux during ecosystem development in montane rain forest. *Ecology* **76**:292–304.

- Robertson, G. P., and J. M. Tiedje. 1984. Denitrification and nitrous oxide production in successional and old growth Michigan forests. *Soil Science Society of America Journal* **48**:383–389.
- Rudolph, J., R. Koschorreck, and R. Conrad. 1996. Oxidative and reductive microbial consumption of nitric oxide in a heathland soil. *Soil Biology and Biochemistry* **28**:1389–1396.
- Runyon, J., R. H. Waring, S. N. Goward, and J. M. Welles. 1994. Environmental limits on net primary production and light-use efficiency across the Oregon transect. *Ecological Applications* **4**:226–237.
- Serca, D., R. Delmas, X. Le Roux, D. A. B. Parsons, M. C. Scholes, L. Abbadie, R. Lensi, O. Ronce, and L. Labroue. 1998. Comparison of nitrogen monoxide emissions from several African tropical ecosystems and influence of season and fire. *Global Biogeochemical Cycles* **12**:637–651.
- Skiba, U., D. Fowler, and K. Smith. 1994. Emissions of NO and N₂O from soils. *Environmental Monitoring and Assessment* **31**:153–158.
- Skiba, U., K. J. Hargreaves, D. Fowler, and K. A. Smith. 1992. Fluxes of nitric and nitrous oxide from agricultural soils in a cool temperate climate. *Atmospheric Environment* **93**:2477–2489.
- Slemr, F., and W. Seiler. 1984. Field measurement of NO and NO₂ emissions from fertilized and unfertilized soils. *Journal of Atmospheric Chemistry* **2**:1–24.
- Smart, D. R., J. M. Stark, and V. Diego. 1999. Resource limitations to nitric oxide emissions from a sagebrush-steppe ecosystem. *Biogeochemistry* **47**:63–86.
- Stark, J. M. 2000. Nutrient transformations. Pages 215–234 in O. E. Sala, R. B. Jackson, H. A. Mooney, and R. W. Howarth, editors. *Methods in ecosystem science*. Springer, New York, New York, USA.
- Stark, J. M., and M. K. Firestone. 1995. Isotopic labeling of soil nitrate pools using nitrogen-15-nitric oxide gas. *Soil Science Society of America Journal* **59**:844–847.
- Stark, J. M., and S. C. Hart. 1996. Diffusion technique for preparing salt solutions, Kjeldahl digests, and persulfate digests for nitrogen-15 analysis. *Soil Science Society of America Journal* **60**:1846–1855.
- Stark, J. M., and S. C. Hart. 1997. High rates of nitrification and nitrate turnover in undisturbed coniferous forests. *Nature* **385**:61–64.
- Venterea, R., and D. E. Rolston. 2000. Mechanisms and kinetics of nitric and nitrous oxide production during nitrification in agricultural soil. *Global Change Biology* **6**:303–316.
- Verchot, L., E. A. Davidson, J. H. Cattanio, I. L. Ackerman, H. E. Erickson, and M. Keller. 1999. Land use change and biogeochemical controls of nitrogen oxide emissions from soils in eastern Amazonia. *Global Biogeochemical Cycles* **13**:31–46.
- Vitousek, P. M., J. R. Gosz, C. C. Grier, J. M. Melillo, and W. A. Reiners. 1982. A comparative analysis of potential nitrification and nitrate mobility in forest ecosystems. *Ecological Monographs* **52**:155–177.
- Williams, E. J., and E. A. Davidson. 1993. An intercomparison of two chamber methods for the determination of emission of nitric oxide from soil. *Atmospheric Environment* **27A**:2107–2113.
- Williams, E., and F. C. Fehsenfeld. 1991. Measurement of soil nitrogen oxide emissions at three North American ecosystems. *Journal of Geophysical Research* **96**:1033–1042.
- Williams, E. J., D. D. Parrish, M. P. Buhr, F. C. Fehsenfeld, and R. Fall. 1988. Measurement of soil NO_x emissions in central Pennsylvania. *Journal of Geophysical Research* **93**:9539–9546.
- Wolf, I., and R. Russow. 2000. Different pathways of formation of N₂O, N₂ and NO in black earth soil. *Soil Biology and Biochemistry* **32**:229–239.